Hydrol. Earth Syst. Sci. Discuss., 8, 5387–5426, 2011
www.hydrol-earth-syst-sci-discuss.net/8/5387/2011/
doi:10.5194/hessd-8-5387-2011
© Author(s) 2011. CC Attribution 3.0 License.

Hydrology and Earth System Sciences Discussions

This discussion paper is/has been under review for the journal Hydrology and Earth System Sciences (HESS). Please refer to the corresponding final paper in HESS if available.

# Effects of freezing on soil temperature, frost propagation and moisture redistribution in peat: laboratory investigations

**R. M. Nagare[1], R. A. Schincariol[1], W. L. Quinton[2], and M. Hayashi[3]**

[1]Department of Earth Sciences, The University of Western Ontario, London, Canada
[2]Cold Regions Research Centre, Wilfrid Laurier University, Waterloo, Canada
[3]Department of Geoscience, University of Calgary, Calgary, Canada

Received: 3 May 2011 – Accepted: 16 May 2011 – Published: 31 May 2011

Correspondence to: R. M. Nagare (rnagare@uwo.ca)

Published by Copernicus Publications on behalf of the European Geosciences Union.





CC BY

## Abstract

The effects of freezing on soil temperature and water movement were monitored in four peat Mesocosms subjected to bidirectional freezing. Temperature gradients were applied by bringing the Mesocosm tops in contact with sub-zero air temperature while maintaining a continuously frozen layer at the bottom (proxy permafrost). Soil water movement towards the freezing front (from warmer to colder regions) was inferred from soil freezing curves and from the total water content of frozen core samples collected at the end of freezing cycle. This study illustrates how differences in initial water content influence the hydrologic functions of active layer in permafrost terrains covered with thick peat during soil freezing. A substantial amount of water, enough to raise the upper surface of frozen saturated soil within 15 cm of the soil surface at the end of freezing period, appeared to have moved upwards during freezing. Effects of temperature on soil matric potential, at least in the initial freezing period, appear to drive such movement as seen from analysis of soil freezing curves. Vapour movement from warmer to colder regions also appears to contribute in moisture movement. Frost propagation is controlled by latent heat for a long time during freezing. A simple conceptual model describing freezing of an organic active layer initially resembling a variable moisture landscape is proposed based upon the results of this study. The results of this study will help in understanding, and ultimately forecasting, the hydrologic response of wetland-dominated terrain underlain by discontinuous permafrost.

## 1 Introduction

Wetland-dominated terrain underlain by discontinuous permafrost covers extensive parts of northern North America and Eurasia. The hydrologic response of these areas is poorly understood, in part due to the lack of understanding of role of individual climatological and soil related factors (e.g., initial moisture conditions) on active layer freeze-thaw processes. The active layer overlies the permafrost and undergoes





HESSD
8, 5387–5426, 2011

seasonal freezing and thawing. Subzero soil temperatures result in higher capillary pressure gradients between warmer and colder regions of frozen soils (Philip and de Vries, 1957). At the onset of winter water from deeper horizons moves toward the freezing front near the ground surface (Dirksen and Miller, 1966; Guymon and Luthin, 1974). Water carries heat and therefore alters both thermal and hydraulic properties of soil during redistribution. Although these processes have been extensively studied in mineral soils (e.g., Dirksen, 1964; Jame, 1978; Hansson et al., 2004), by comparison only a few studies have examined moisture redistribution in organic soils (e.g., Carey and Woo, 2005; Quinton et al., 2005). Peat can have bulk densities ($\rho_b$) as low as 0.035 kg m$^{-3}$ and porosities sometimes exceeding 96 % by volume. These characteristics are common in the peat deposits at or near the ground surface (e.g., Schlotzhauer and Price, 1999; Quinton et al., 2009). The high porosities results in significant changes in the thermal and hydrological properties of peat as soil water content varies (de Vries, 1963; Smerdon and Mendoza 2010).

In organic-covered permafrost terrain, the topography of the relatively impermeable frost table plays an important role in controlling spring runoff (Wright et al., 2009). It is broadly understood that factors such as climate, canopy cover, ground slope, and soil moisture and thermal properties of soil play critical roles in development or degradation of permafrost. Redistribution of moisture within the active layer during the winter months plays an important role in determining the position of the impermeable frost table at the onset of end-of-winter snowmelt event. The mechanisms that drive this redistribution of moisture are poorly understood (Quinton and Hayashi, 2008). For example, observations of Quinton and Hayashi (2008) suggest that at onset of winter, the water table is typically deeper than 0.5 m below ground, while at the start of spring melt, the upper surface of the frozen, saturated soil is typically about 0.1 m below the ground surface. How this condition developed during the winter period remains unclear. Field investigations by Quinton and Hayashi (2008) suggest that the amount of water supplied to the soil during the spring melt event in addition to the cumulative amount of meltwater supplied during over-winter melt events, is sufficient to saturate





CC BY

the ∼0.4 m thick soil zone between the water table position at the time of freeze-up and the frost table position at the end of winter. The role latent heat plays in the propagation of frost has been examined (e.g., Harris et al., 2008), yet the effect of different soil moisture conditions on frost propagation and frost induced water redistribution remains unclear. Soil moisture profile at the onset of winter also governs the ice content in the surface layer of the organic soils. The rate of thaw propagation is affected by the initial soil ice content. Once thaw reaches a certain depth infiltration into organic soils becomes unlimited (Gray et al., 1985, 2001). Field studies have greatly contributed to advancing the understanding of freeze-thaw processes in organic terrains (e.g., Quinton et al., 2005; Carey and Woo, 2005). However, seasonal limits on the accessibility of field sites mean that laboratory and numerical studies are required to develop and complement the fundamental understanding of freeze-thaw and moisture distribution processes that occur throughout the year. Mathematical theories and improved numerical approaches (e.g., Hansson et al., 2004; Dall'Amico et al., 2010) are still being developed to increase the efficiency of modeling approaches.

Soil column and lysimetric experiments, under controlled laboratory conditions, produce data that can be used to verify these models. Examples of column experiments to study coupled water and heat movement in frozen mineral soils can be found in literature (e.g. Dirksen, 1964; Hoekstra, 1966; Jame, 1978; Guymon et al., 1993, Stahli and Staedler, 1997; Gergely 2007). However, two major limitations in using this experimental data involve realistic boundary conditions and soil heterogeneity. Soil column freeze-thaw experiments have been traditionally conducted with cold plates at least at one end (e.g., Mizoguchi, 1990; Jame, 1978; Stahli and Staedler, 1997; Gergely 2007). In these experiments the other end of the column was either thermally insulated, in contact with a warm/cold plate, or exposed in a freezer/cold room. This does not create realistic replication of field permafrost conditions or the bi-directional freezing of the active layer, and hence, the influence of subsurface thermal properties on near surface energy balance is not the same. Laboratory studies using uniformly packed soil columns subjected to simplified boundary conditions have long been used to verify





CC BY

numerical schemes and mathematical theories (e.g., Jame and Norum, 1980; Hansson et al., 2004; Painter, 2010). Zhang et al. (2010) point to limitations of schemes verified with such data when applied to non-uniform/ layered soil conditions, or large flux conditions such as snow melt infiltration. Data for such verification cases is scarce and experiments under controlled laboratory settings need to be aimed at observing freeze-thaw processes that emulate field conditions as closely as possible (e.g., undisturbed soil cores) with realistic boundary conditions.

Innovative experimental design is required to isolate the influence of individual climatological factors, soil moisture conditions and soil properties on soil freezing and thawing. This study uses four mesocoms that are thermally insulated on the sides and contain a basal layer of peat that is continuously frozen to simulate permafrost (proxy permafrost). The air above the Mesocosms was maintained at temperatures below 0 °C so that the unfrozen peat above the simulated permafrost could be subjected to bidirectional, one-dimensional freezing. The influence of initial soil moisture on freezing processes was studied by maintaining the four Mesocosms at different water contents at the start of freezing. The experiments were specifically aimed at:

1. observing the process of freezing-induced soil water redistribution, and the role of the initial soil water content in movement of water towards the freezing fronts. Correlating the freezing-induced soil water redistribution to the over-winter moisture redistribution observed in the field is needed to understand the over-winter moisture redistribution processes that result in the saturation of most of the active layer by the end of winter;

2. understanding if the initial soil moisture profile governs the ice content in the peat near the ground surface, which has implications for the partitioning of snowmelt water into infiltration and runoff.

3. understanding the effects of initial water content on (a) soil freezing characteristics; and (b) soil thermal properties and frost propagation.





HESSD
8, 5387–5426, 2011



CC BY

4. organizing the observations of this study into a simple conceptual model to describe the processes of freezing front movement and freezing induced water redistribution.

## 2 Methodology

### 2.1 Experimental setup

The experimental setup consisted of four peat Mesocosms (M1, M2, M3 and M4), each ∼110 cm deep and 56 cm in diameter. All Mesocosms consisted of a ∼45 cm thick proxy permafrost layer prepared by packing unprocessed humified peat to a bulk density of ∼250 kg m$^{-3}$. Once prepared, this layer was completely saturated and allowed to freeze at −6 °C. Intermediate layers of unprocessed humified peat were then packed in each Mesocosm (bulk density varying from ∼250 kg m$^{-3}$ to ∼125 kg m$^{-3}$) to a thickness that allowed ∼110 cm deep Mesocosms to be formed when the undisturbed field sampled cores were placed over these layers (Table 1). The unprocessed humified peat used for proxy permafrost and intermediate layers was obtained from the Upsala, Ontario operations of Peat Resources Ltd. The undisturbed cores were extracted from Scotty Creek watershed, Northwest Territories, Canada in the wetland-dominated, discontinuous permafrost. Details of the site location, landform types and site characteristics can be found in Quinton et al. (2008), and details of coring methodology can be found in Nagare et al. (2011b). Dry bulk densities and porosities for Scotty Creek peat were reported by Hayashi et al. (2007) and are shown in Fig. 1a and b. The vertical hydraulic conductivity of saturated peat was measured for different depths in the laboratory using the cube method (Fig. 1c). Water retention characteristics for the peat layers were reported by Quinton and Hayashi (2005) as shown in Fig. 1c. In general, deeper peat layers hold more water at higher tension. For peat from the same site, Rezanezhad et al. (2009) found the degree of humification on the von Post scale to change from H3 just below surface vegetation to H5 at a depth of 65 cm.

The Mesocosms were setup in the Earth Science module (BESM) of the Biotron Institute for Experimental Climate Change at the University of Western Ontario. The BESM is a two level biome with four dedicated compressors, two each for the upper and lower chambers with an air temperature control range of −40 °C to +40 °C. By situating the Mesocosms between these two chambers it was possible to maintain a frozen state in the lower ~45 cm of the core while allowing for freezing and thawing of the overlying peat. Light intensity, rain, relative humidity, wind speeds, and $CO_2$ concentrations can be controlled independently in upper chamber. Further details on the BESM facility can be found in Nagare et al. (2011b).

Mesocosms were instrumented at different depths with time domain reflectometry (TDR) sensors (TDR100, CS610 and CS635 probes, Campbell Scientific, Inc., Logan UT) and temperature sensors (107BAM, Campbell Scientific, Inc., Logan UT). A heat flux plate each (HFT3, Campbell Scientific, Inc., Logan UT) was inserted near the soil's surface in M2 and M3. Sampling ports were drilled in the sides of the Mesocosms at different depths to allow soil gas and water sampling. The Mesocosms were placed on four 81 cm × 81 cm load cells (KC600S, 10 g precision over 600 kg, Mettler Toledo Canada, Mississauga, ON) for continuous weighing such that the bottom ~45 cm of the Mesocosms were the in lower chamber and the remainder protruded into the upper chamber. The sides of the Mesocosms were insulated using a combination of neoprene foam and mineral fibre insulation. The lower chamber was maintained at −1.9 °C to keep the bottom ~45 cm of the cores continuously frozen while the air temperature was varied in the upper chamber. Figure 2 shows a schematic of the experimental setup with detailed explanation of various components. Soil dielectric permittivity, temperature, heat flux and weight were recorded every 15 min.

### 2.2 Experimental conditions

Two freezing runs were conducted. In the first run, the Mesocosms were subjected to air temperature in the upper chamber of −5 °C for 31 days and then −10 °C in the following 16 days. This first run was aimed at understanding the freezing characteristics





CC BY

in general. All four Mesocosms had an unfrozen, saturated layer at the commencement of the first freezing run with water table depths of 27-, 43-, 40- and 32 cm below the surface respectively. To establish saturated layers within the Mesocosms, water was sprayed daily (twice a day in different amounts) on the surface and the Mesocosms were allowed to equilibrate for at least 30 days. After 47 days of freezing, it took 75 days to thaw the active layer down to the top of the proxy permafrost layer. The air temperature in the upper chamber was maintained constant at 15 °C and lights (wavelength: 400–750 nm) were kept on such that the soil surface level received an energy input of 160 W m$^{-2}$. A further 75 days were required to establish the initial conditions for the second freezing run. The air temperature in the upper chamber was maintained at −7.5 °C for 93 days during the second freezing run. The air temperature in the lower chamber was kept constant at −1.9 °C. Most of the data from first freezing run could not be used because of sequential failure of temperature sensors during this run. Therefore, soil freezing characteristics and influence of initial water content on soil water redistribution and frost propagation was examined from the data of the second freezing run.

## 2.3 TDR calibration

A detailed calibration of the TDR100 was performed by Nagare et al. (2011a) at a constant temperature (30 °C) using undisturbed peat samples from the Scotty Creek field site. In an independent test, Nagare et al. (2011a) also determined the temperature dependency of the observed apparent dielectric permittivity ($\varepsilon$) of unfrozen peat-air-water mixture at three different volumetric water contents ($\theta$) as shown in Fig. 3a. It can be seen that $\varepsilon$ is significantly affected by temperature at higher water contents. Figure 3b shows the relationship between temperature and $\varepsilon$ for water (unfrozen and frozen states) in the −10 °C to +16 °C range. The same relationship was observed by Wohlfarth (2010). Neither peat nor air shows any variation in $\varepsilon$ with changing temperature (Fig. 3c). The increase in $\varepsilon$ with decreasing temperature for the peat-air-water mixture can be thus solely attributed to the temperature-$\varepsilon$ relationship of water. The




CC BY

apparent dielectric permittivity of ice remains close to 3.14 without any dependency on decreasing temperature in the observed range (Fig. 3b). Maxwell De-Loor's (MDL) mixing model can efficiently handle the temperature effects on the $\varepsilon-\theta$ relationship Nagare et al. (2011a). Because a temperature correction is required for the empirical equation, the MDL model was used to estimate water content from observed $\varepsilon$ in the mesocom experiments after calibrating it with the empirical equation at 30 °C. Bound water was not taken into account and the influence of ice on apparent dielectric permittivity was not considered owing to the inability of estimating pore ice content.

### 2.4 Final total water content

Final total water content (ice + liquid water) was measured at the end of the second freezing run for all four Mesocosms. Cores were extracted from the frozen Mesocosms using a custom designed coring tool (30 cm long thin walled stainless steel tube; 2.03 cm inner diameter) powered by an electric drill. Two cores each from M2 and M4 were sampled from depth intervals 0–25 cm and ~25–45 cm by slowly drilling into the samples in two depth increments. Two cores between depth intervals 0–25 cm and ~25–36 cm could be extracted from M1. The final water content in M3 could be determined only for the upper 9.1 cm, as efforts to core deeper in this Mesocosm did not succeed due to high ice contents. The cores were cut while frozen into smaller sections, weighed and oven dried at 87 °C until no further change in weight was recorded. The dry samples were weighed again for gravimetric measurement of the final total water content.

The cores were extracted near the edges of the Mesocosms. Although it is best to determine total water content at different depths for entire soil column, it was not possible in our case as we continued using the Mesocosms for further research on freezing and thawing processes in peat. Extracting cores near edge may have resulted in relatively unrealistic final total water contents possibly because of different flow regimes near column edges, lateral heat leak effects and lateral redistribution of water within the Mesocosms. However, in this study the data from the cores is assumed to be good enough for the purpose of process based discussion.

## 3 Results and discussion

### 3.1 Initial conditions

The influence of water content at the start of the freezing run on active layer freezing processes was studied during the second freezing run. Figure 4 shows the initial water content profiles in all four Mesocosms at the start of the second freezing run. Initial water content is the unfrozen water content at the start of the freezing run estimated from TDR observations. Mesocosms 1 and 4 were variably saturated at the start of this freezing run with the water tables located at 42 cm and 27 cm below the ground surface respectively. Mesocosm 2 was variably saturated throughout the depth with no saturated zone, while the water table was located at ~5.5 cm in Mesocosm 3 at the start of the freezing run. A linear initial temperature profile in each Mesocosm was achieved by maintaining the air temperatures in lower and upper chambers at −1.9 °C and 3 °C respectively until a relatively stable linear profile was achieved.

### 3.2 Soil freezing characteristics

Soil freezing characteristics (SFCs) at different depths were determined from observed liquid water content and soil temperature data collected during the second freezing run. Water in M1, M2, M3 and M4 started to freeze at −0.08 °C, 0 °C, −0.05 °C and −0.08 °C respectively, and represent the temperatures at which peat water starts to freeze (freezing point before further depression) in each Mesocosm in the discussion to follow (Fig. 5). It is evident that some water remained unfrozen even after 2000 h (83 days) of freezing (Fig. 6a) with residual liquid water contents between 0.05 $m^3\,m^{-3}$ and 0.13 $m^3\,m^{-3}$ continuing to exist even at −5 °C. Shallower depths are left with less





CC BY

residual water than deeper ones for the same freezing temperatures. Similarly, depths with higher initial water contents are left with slightly larger amounts of residual water at similar temperatures. A few SFCs in all Mesocosms appear to be affected by water redistribution at some stage for temperatures below freezing (Fig. 7). However, overall the other SFCs appear to follow a common path during freezing. As theorized by Low et al. (1968), liquid water content in frozen soils must have a fixed value for each temperature at which the liquid and ice phase are in equilibrium, regardless of the amount of ice present. It is convenient to define a single soil freezing curve for a particular soil type in order to simplify the relationship between soil temperature and liquid water content. An example of a single curve defining the temperature-liquid water content relationship based on the van Genuchten model (van Genuchten, 1980) is shown in Fig. 8. The curve was obtained by fitting into the soil temperature and liquid water content data other than those shown in Fig. 7. This approximation of the SFCs in a single curve is important for numerical studies as it simplifies the constitutive relationship between soil temperature and liquid water content.

### 3.3 Frost induced water redistribution within the active layer

Soil water redistribution during the second freezing run in each Mesocosm was inferred based on initial and final total water contents and SFCs at different depths.

*Variably saturated conditions with a water table at depth (Mesocosms 1 and 4)*: In both M1 and M4 the zone near and above the water table loses water because of movement upwards towards the freezing front before the soil temperature falls below the freezing point. This movement is evident from the reduction of water content at 15 cm and 25 cm depths prior to soil freezing (Figs. 5a and d). Before the arrival of freezing front, the reduction in water content ranges from ~0.27 $m^3\,m^{-3}$ at 25 cm depth in M4 to ~0.07 $m^3\,m^{-3}$ in M1. This difference appears to have resulted from the higher water content in the top 10 cm of M4 and therefore higher hydraulic conductivity than in M1. Figure 9 shows the effect of freezing on water redistribution in Mesocosm M4. The



HESSD
8, 5387–5426, 2011

Lab investigation of freezing processes in peat

R. M. Nagare et al.

freezing front descends from the surface and arrives at 5 cm in M4 after ~69 h. At this time, the slope of the SFC at 25 cm depth becomes steeper illustrating a higher rate of moisture flow toward the overlying peat. Freezing reduces the soil pore pressures significantly due to changes in surface tension, temperature sensitivity of contact angles and the increase in volume as water transforms to ice (Philip and de Vries, 1957; Grant and Bachmann, 2002) creating large pore pressure gradients between the colder and warmer regions. The loss of water from 25 cm depth interval in M4 prior to 69 h (and beyond) must have resulted from potential gradients created between the surface, where the temperature drops below zero within first few hours, and deeper depths. A reduction in water content was observed in both M1 and M4 prior to the temperature falling to freezing point. However, it appears that hydraulic conductivity differences due to differences in initial water contents in the upper 10 cm of these two Mesocosms play a role during upward movement of water from 15 cm depth. No water movement is observed from 15 cm depth in M1 until 43 h into the freezing run, while water movement from the same depth in M4 starts within the first hour of the ground surface freezing (Fig. 10). Water from 15 cm depth in M1 migrates upwards only after the downward propagating freezing front has reached between 5 cm and 10 cm creating a hydraulic gradient steep enough for water movement to occur. The shapes of the SFCs at 37 cm in M1 and 52 cm in M4 indicate that water migration continues late into the freezing run and that these depths are gaining and losing water as the upper freezing front moves downward.

*Dry conditions (Mesocosm 2)*: Mesocosm 2 was the driest among the four at the start of second freezing run with only residual water contents in upper 30 cm (~0.15 $m^3\ m^{-3}$ at 28 cm, Fig. 4b), had no saturated layer and had a degree of saturation of ~50 % at 55 cm. No reduction of water content was observed in M2 at temperatures above freezing (Fig. 5b). This can be attributed to extremely low hydraulic conductivities in the dry zone. The frost penetration in the upper 30 cm of this Mesocosm was relatively rapid and steeper hydraulic gradients appear to have been created.





HESSD
8, 5387–5426, 2011

*Saturated conditions (Mesocosm 3)*: At the start of the freezing run, the water table in M3 was at ~5.5 cm. It is difficult to infer any water movement for this Mesocosm from SFC alone, except at 5 cm depth, where water loss commenced prior to the temperature falling below freezing.

There is a good match between the arrival time of the freezing front at a shallower depth and migration of water from a deeper depth as seen in Fig. 9. This illustrates the importance of soil freezing on the matric potential at least in the initial freezing period (e.g., water removal prior to freezing front reaching 25 cm depth in M4 continued for first 281 h as seen in Fig. 9. The generalized Clausius-Clapeyron equation (CCE) is used to convert from temperature to matric potential in frozen soils. There have been very few efforts (e.g., Williams, 1967; Guymon et al., 1993) to measure soil matric potential in frozen soils owing to the difficulties in using the existing measuring techniques. While there are very few experimental works verifying the use of CCE in frozen soils, Williams (1967) show a close match between the observed and predicted values of matric potential in a Leda Clay-water-ice system. The effect of temperature on matric potential needs to be further examined and extended to peat in order to improve the numerical support in cold regions water balance studies.

The final water content profiles indicate an upward water movement in all Mesocosms (Fig. 11), although the rates of water flow appear to have varied among the Mesocosms owing to the differences in initial moisture profiles and moisture dependant hydraulic conductivities. The role of hydraulic conductivity is evident from the differences in the final total water content profiles of M1 and M4. M1 had less water in the upper 10 cm and water accumulated behind this low permeability zone. In comparison, there was a more gradual change toward the final water content profile of M4. Most water can be observed to be lost from the zone just above water table in both M1 and M4. The role of hydraulic conductivity can also be seen from the comparison between the soil freezing curves of M1 and M4 at 15 cm depths (Fig. 10). Water coming from the deeper depths accumulated just above the 15 cm depth in M1 (Fig. 11a). The shape of the SFC at 15 cm in this Mesocosm is clearly affected by the water coming from deeper





CC BY

depths. In comparison, the SFC at 15 cm in M4 was not affected as much because water may have moved through this zone at a much faster rate owing to comparatively higher hydraulic conductivity in the zone above.

The movement of water towards freezing front appears to have been dominated by liquid water movement under potential gradients at least in the initial freezing period. However, there is enough indication that moisture movement also took place in vapour form. The weights of the Mesocosms continued to drop during the freezing period (not shown). This indicates that water was escaping from the Mesocosms during freezing. This is an evidence of water transport in vapour form from warmer regions with high water contents towards colder regions with relatively low water contents. The modes of transport and quantification of contribution from liquid water movement and vapour transport are a topic of further investigation and will be discussed in a separate publication in near future.

One critical issue in field studies is to understand the role of over-winter snowmelt events, and the origin of water participating in the freezing of active layer over the winter season. Figure 12 shows the water content values observed at the Scotty Creek research site at beginning and end of winter season of 2002–2003. Initial moisture conditions for the field were not measured below 40 cm. The depth to permafrost at the onset of winter was 70 cm. This site is underlain by sporadic/discontinuous permafrost (Smith et al., 2004; Quinton and Hayashi, 2005).

It is evident that a large amount of water moved into 0–40 cm depths at the end of the winter (Fig. 12). Comparing Figus. 11 and 12 indicates that it is possible that water from deeper zones at initial high water contents moved upward towards the freezing front during the winter season and resulted into the final profiles in Fig. 12. The measurements in Fig. 12 indicate a 41.85 mm change in storage in the upper 40 cm depth. A change of storage of 33.65 mm and 42.11 mm in upper 29 cm and 21 cm in M1 and M4 respectively was inferred from the initial and final profiles (Fig. 11). It must be noted that the initial water content in upper 40 cm depth in both Mesocosms (Fig. 4) was higher than the initial water content in the field (initial moisture in Fig. 12). Also, the water table was within upper 40 cm depth in both Mesocosms and the air temperature at the surface was constantly at −7.5 °C. All these conditions may have resulted into relatively larger amount of water movement towards the freezing front in the Mesocosms than in the field. This is an important observation as it suggests that temperature gradients drive an upward flux of water from deeper regions of the soil into the upper 10 cm zone where it can be supplemented by an intermittent downward flux of snowmelt water over the winter period. This combination of freezing induced upward migration of water supplemented by an intermittent downward flux of snowmelt water over the winter period results into raising the upper surface of the frozen, saturated soil typically within about 0.1 m below the ground surface.

### 3.4 Soil temperature and frost propagation

Figure 13 shows the isothermal maps for all four Mesocosms plotted from temperature measurements during the second freezing run. Bi-directional freezing, with a relatively fast moving downward and a slower moving upward freezing front, can be observed in all four Mesocosms. The freezing front propagates faster and deeper in upper dry ∼35 cm of M2 due to minimal latent heat release. Freezing slows down considerably below this depth due to relatively high saturation and latent heat effects. Strong thermal gradients can be seen near surface in the wetter M1, M3 and M4 Mesocosms indicating presence of high amounts of water near the freezing front. In all four Mesocosms, the frost propagation is controlled by competing roles of thermal diffusivity and latent heat. The slow progression of the freezing front in M2 below the upper 30 cm is due to a combination of latent heat, and low thermal conductivity owing to drier peat and higher air volume relative to M1, M3 and M4. The role of thermal conductivity in the ground heat removal can be seen from the difference in ground heat flux (from heat flux plates) observations between Mesocosms M2 and M3 (Fig. 14a). It can be seen that the heat removed from the saturated Mesocosm M3 is consistently higher than from the dry M2. Most water in Mesocosms M1, M3 and M4 freezes around ∼2000 h (Fig. 6a) after which the freezing front propagates deeper and at a higher rate. Thus, latent heat plays a significant role in keeping the soil warm, yet higher water contents result in colder horizons at depths owing to higher thermal conductivity and lower heat capacity during late freezing periods.

The effect of differences in sub-surface thermal properties on near surface thermal regimes can be seen from comparison between the Mesocosms with colder (M1) and warmer (M4) proxy permafrost. Figure 14b shows the time series of temperature changes of near surface depths in these Mesocosms. Both M1 and M4 were variably saturated throughout the depth with water tables located at 42 cm and 26 cm below the ground surface at the start of freezing. Mesocosm 4 was relatively wetter than M1 in the upper 10 cm when freezing commenced, and had a warmer proxy permafrost (−0.35 °C) than M3 (−0.88 °C). Although both Mesocosms were subjected to the same air temperature in the lower chamber, the differences in temperatures of the proxy permafrost were probably due to differences in water contents. The colder proxy permafrost resulted in a greater ice content in M1 compared to soils at similar depths in M4. The comparison of temperature at similar depths in these two Mesocosms reveal that the temperature time series of M4 always lags M1 in reaching the −0.08 °C line (freezing point for these two Mesocosms). A higher ice content in M1 resulted in a higher thermal conductivity and lower heat capacity than M4 and thus results in quicker heat loss.

The results of this study are used to describe the evolution of frost table topography for a peat plateau through a simple conceptual model (Fig. 15). The model is hypothetical, but it provides a useful framework for discussion. At the onset of winter, the organic active layer resembles a variable moisture landscape with regions of full saturation under the topographic depression, low moisture content (at the top with a dry surface layer), and relatively wetter unsaturated zone below the dry surface layer and under the mound. The water table more or less resembles the surface topography. When the air temperatures drop below freezing, the freezing front migrates at variable rates in the different regions. The rate of migration in early winter is maximum in the dry surface layer because there is very little moisture to slow down the descend (Fig. 15b).





HESSD
8, 5387–5426, 2011



cc BY

In comparison the rate of freezing front movement is slowest under the topographic depression where peat is fully saturated. Water from the regions just above the water table moves upward in response to the pressure head gradient created between the colder and warmer regions drawing the water table downward. Water also moves in form of vapour during this period, however liquid water movement under pressure head gradients is possibly the dominant process in initial periods. As the winter progresses, so does the freezing front drawing more water from regions of higher saturation creating a continuous zone of increased saturation just below it (Fig. 15c). Much more water is accumulated behind the freezing front in regions where the initial water content in unsaturated zone was relatively high (e.g., under the mound higher rate of water flow is shown by longer arrow). This happens because of the higher hydraulic conductivity of the wetter unsaturated zones as compared to the drier ones. In comparison, the initially dry surface layer remains on lower side of saturation because the low hydraulic conductivity in this layer slows down the upward movement of water beyond its interface with the wetter unsaturated zone underneath. By mid-winter (Fig. 15d), there is no more a saturated unfrozen zone on the entire peat plateau. The entire plateau is unsaturated because of freezing induced water redistribution or partial freezing of soil water. The soil moisture migration (liquid + vapour) towards freezing front continues from areas where there is still substantial liquid water. As the water accumulating behind the freezing front freezes, it also retards the movement of the freezing front (Fig. 15c and d). The rate of descend still is slowest below the topographic depression and the mound where maximum water is accumulating behind the freezing front. By mid to late winter (Fig. 15e and f), most of the water behind the freezing front is frozen, except under the topographic depression and the mound. Elsewhere on the peat plateau, the downward freezing front movement accelerates. By this time, freezing induced water movement has slowed down considerably except near the depression where larger effects of temperature on soil matric potential (because of higher ice content than elsewhere) and initially high hydraulic conductivity still result into comparatively higher rate of upward water redistribution. As most water freezes behind the freezing front, the front migrates much more rapidly owing to increased thermal conductivity and lower release of latent heat. By the end of winter most water redistribution stops and the entire soil profile is now below freezing temperatures with warmest temperatures occurring at depths. The significant water movement upwards in early to mid, late-mid winter periods results into a continuous saturated frozen layer near surface of varying thickness. The thickness is minimum below the dry surface layer and maximum below the topographic depression and the mound. This saturated frozen layer creates a near impermeable frost table near surface with variable thickness of unsaturated zone above it. As spring arrives and snow melts, runoff takes place in different modes in different regions of the peat plateaus. There is unimpeded infiltration into the dry surface layer with lowest ice content. The infiltrating water runs off down-slope along the topography of the frost table through the subsurface. Near the topographic depression and the mound, where the impermeable surface is flush with ground surface, most snowmelt runoff takes place as overland flow along the topographic slopes.

## 4 Conclusions and implications

Four peat Mesocosms with different initial moisture contents were subjected to freezing to study the impact of soil water content on soil freezing characteristics, freezing induced soil water redistribution, and frost penetration.

There appears to be very little effect of initial soil moisture on soil freezing characteristics of peat. This implies that liquid water content in frozen peat has a fixed value for each temperature at which the liquid and ice phase are in equilibrium, regardless of the amount of ice present. A single freezing curve can be derived, regardless of initial soil moisture. This simplifies the temperature-liquid water content parameterization required for numerical studies. Initial moisture profiles seem to control the amount of water moving upwards by influencing the hydraulic conductivities in variably saturated media. Substantial water redistribution appears to have taken place within the active layer during its freezing. This suggests that in favorable conditions the water moving from deeper depths under temperature gradients, with “complementary” contribution from preceding over-winter melt events, could be sufficient to raise the upper surface of frozen saturated soil within upper 10 cm zone. Effects of temperature and phase change on soil matric potential appear to be the primary cause behind the movement of water towards the freezing front in initial freezing periods, while vapour movement from warmer wetter regions towards colder drier regions also appears to play a role in water movement. Initial water content in the surface layer (∼10 cm) appears to control the amount of ice and location of the zone where maximum ice is formed near the surface. It appears that if there is a relatively thick dry layer, then water moving towards the freezing front from below is accumulated relatively at a deeper depth as compared to if the surface layer was moist. Also, the ice content in a dry surface layer would be much lower than a relatively wetter surface layer. This has implications in the timing and mode of runoff during the initial thaw period because an initially dry surface layer would result into unimpeded higher infiltration.

The frost movement in the four Mesocosms with different initial moisture content shows that frost propagation in frozen soils is controlled by a combination of latent heat and thermal properties of the peat-air-water-ice system. Latent heat governs the frost propagation for a long time during freezing because of high water contents in peat. Once water in peat is frozen, higher thermal conductivity and lowered heat capacity of frozen peat-ice system helps in faster movement of the frost front. Climate change scenarios predict shorter periods of snow cover in northern latitudes (Serreze et al., 2000; IPCC, 2007). This will increase the rate of freezing of peat pore water. If the peat contains substantial water at the onset of winter, then this might lead into deeper frost depths. Mean annual air temperature and rainfall in the northern hemisphere are also predicted to increase (Serreze et al., 2000; IPCC, 2007). A system with competing dynamics of frost penetration due to longer ground exposure to winter air temperatures and overall higher annual mean air temperature forcing deeper permafrost appears to be a possible scenario.

This study demonstrates that soil moisture profiles at the onset of winter play an important role in modulating the hydraulic and thermal properties of peat and therefore





CC BY

affecting the frost induced water redistribution and frost propagation during the freezing of active layer. For example, the results of this study are in agreement with the modeling study of Jorgenson et al. (2010) in which the modeled temperatures for permafrost overlain by dry organic mats was found to be much colder than for wet overlying mats. The results of this study will help in understanding, and ultimately forecasting, the seasonal freeze-thaw hydrologic response of wetland-dominated terrain underlain by discontinuous permafrost. Further research through numerical modeling and laboratory work involving experimental design similar to that of this study is required to understand the exact impacts of the competing dynamics driving the water and heat movement in frozen peat.

*Acknowledgements.* We wish to acknowledge the financial support of the Natural Science and Engineering Research Council (NSERC) and BioChambers Inc. (MB, Canada) through a NSERC-CRD award, NSERC Strategic Projects grant, and the Canadian Foundation for Climate and Atmospheric Sciences (CFCAS) through an IP3 Research Network grant. We also thank Andrea Kenward, Trevor Meyers and Pete Whittington for their assistance in the field, and acknowledge the help of Frank Van Sas, Brian Dalrymple, Jonathan Jacobs, Jeremy Bird and Jalpa Pal in setting up the Mesocosm experiment. We acknowledge the Aurora Research Institute for their assistance in obtaining a research license, and thank the Denedeh Resources Committee, Deh Cho First Nation, Fort Simpson Métis Local #52, Liidlii Kue First Nation, Jean-Marie First Nation and the Village of Fort Simpson for their support of this project.

## References

Carey, S. K. and Woo, M. K.: Freezing of subarctic hillslopes, Wolf Creek basin, Yukon, Canada, Arct. Antarct. Alp. Res., 37, 1–10, 2005.

de Vries, D. A.: Thermal Properties of Soils, in: Physics of Plant Environment, edited by: van Wijk, W. R., North-Holland Pub. Co., 210–235, 1963.

Dall'Amico, M.: Coupled water and heat transfer in permafrost modeling, Ph.D thesis, University of Trento, 2010.

Dirksen, C. and Miller, R. D.: Closed-System Freezing of Unsaturated Soil, Soil Sci. Soc. Am. Pro., 30, 168–173, 1966.





HESSD

8, 5387–5426, 2011

Dirksen, C.: Water Movement and Frost Heaving in Unsaturated Soil without an External Source of Water, Ph.D. thesis, Cornell University, United States – New York, 152 pp., 1964.

Gergely, M.: Dynamics of a salty permafrost, M.Sc. thesis, University of Heidelberg, Germany, 2007.

Grant, S. A. and Bachmann, J.: Effect of temperature on capillary pressure, Geophysical Monograph, American Geophysical Union, 129, 199–212, 2002.

Gray, D. M., Landine, P. G., and Granger, R. J.: Simulating Infiltration into Frozen Prairie Soils in Streamflow Models, Can. J. Earth Sci., 22, 464–472, 1985.

Gray, D. M., Toth, B., Pomeroy, J. W., Zhao, L., and Granger, R. J.: Estimating areal snowmelt infiltration into frozen soils, Hydrol. Process., 15, 3095–3111, 2001.

Guymon, G. L., Berg, R. L., and Hromadka, T. V.: Mathematical Model of Frost Heave and Thaw Settlement in Pavements, US Army Corps Cold Regions Research & Engineering Laboratory, 130 pp., 1993.

Guymon, G. L. and Luthin, J. N.: Coupled Heat and Moisture Transport Model for Arctic Soils, Water Resour. Res., 10, 995–1001, 1974.

Hansson, K., Simunek, J., Mizoguchi, M., Lundin, L. C., and van Genuchten, M. T.: Water flow and heat transport in frozen soil: Numerical solution and freeze-thaw applications, Vadose Zone J., 3, 693–704, 2004.

Harris, C., Arenson, L. U., Christiansen, H. H., Etzelmuller, B., Frauenfelder, R., Gruber, S., Haeberli, W., Hauck, C., Hoelzle, M., Humlum, O., Isaksen, K., Kaab, A., Kern-Luetschg, M. A., Lehning, M., Matsuoka, N., Murton, J. B., Noezli, J., Phillips, M., Ross, N., Seppala, M., Springman, S. M., and Muehll, D. V.: Permafrost and climate in Europe: Monitoring and modelling thermal, geomorphological and geotechnical responses, Earth-Sci. Rev., 92, 117–171, doi:10.1016/j.earscirev.2008.12.002, 2009.

Hayashi, M., Goeller, N., Quinton, W. L., and Wright, N.: A simple heat-conduction method for simulating the frost-table depth in hydrological models, Hydrol. Process., 21, 2610–2622, doi:10.1002/hyp.6792, 2007.

Hoekstra, P.: Moisture Movement in Soils Under Temperature Gradients with Cold-Side Temperature Below Freezing, Water Resour. Res., 2, 241–250, 1966.

IPCC, 2007. Climate Change 2007: The Physical Science Basis. Contribution of Working Group I to the *Fourth Assessment Report of the Intergovernmental Panel on Climate Change*, edited by: Solomon, S., Qin, D., Manning, M., Chen, Z., Marquis, M., Averyt, K. B., Tignor, M., and Miller, H. L., Cambridge University Press, Cambridge, United Kingdom and New York, NY,





CC BY

USA 2007.
Jame, Y.: Heat and Mass Transfer in Freezing Unsaturated Soil, Ph.D. thesis, The University of Saskatchewan (Canada), Canada, 212 pp., 1978.
Jame, Y. W. and Norum, D. I.: Heat and Mass-Transfer in a Freezing Unsaturated Porous-Medium, Water Resour. Res., 16, 811–819, 1980.
Jorgensen, M. T., Romanovsky, V., Harden, J., Shur, Y., O'Donnell, J., Schuur, E. A. G., Kanevskiy, M., and Marchenko S.: Resilience and vulnerability of permafrost to climate change, Can. J. For. Res., 40, 1219–1236, 2010.
Low, P. F., Anderson, D. M. and Hoekstra, P.: Some Thermodynamic Relationships for Soils at Or Below Freezing Point 1. Freezing Point Depression and Heat Capacity, Water Resour. Res., 4, 379–394, 1968.
Mizoguchi, M.: Water, heat and salt transport in freezing soil, Ph. D thesis, University of Tokyo, Tokyo, 1990.
Nagare, R. M., Schincariol, R. A., Quinton, W. L., and Hayashi, M.: Laboratory calibration of time domain reflectometry to determine moisture content in undisturbed peat samples, European J. of Soil Sci., in press, 2011a.
Nagare, R. M., Schincariol, R. A., Quinton, W. L., and Hayashi, M.: Moving the field into the lab: Simulation of water and heat transport in sub-Arctic peat, Permafrost Periglacial Processes, in review, 2011b.
Painter, S.: Three-phase numerical model of water migration in partially frozen geological media: model formulation, validation, and applications, Computational Geosciences, 1–17, doi:10.1007/s10596-010-9197-z, 2010.
Philip, J. R. and de Vries, D. A.: Moisture movement in porous materials under temperature gradient, Transactions, American Geophysical Union, 38, 222–232, 1957.
Quinton, W. L. and Hayashi, M.: The flow and storage of water in the wetland-dominated central Mackenzie river basin: Recent advances and future directions, in: Prediction in ungauged basins: Approaches for Canada's cold regions, edited by: Spence, C., Pomeroy, J. W., and Pietroniro, A., Canadian Water Resources Association, 45–66, 2005.
Quinton, W. L. and Hayashi, M.: Recent Advances Toward Physically-based Runoff Modeling of the Wetland-dominated Central Mackenzie River Basin, in: Cold Region Atmospheric and Hydrologic Studies, edited by: Woo, M., The Mackenzie GEWEX Experience: Volume 2: Hydrologic Processes, Springer, Berlin, 257–279, 2008.
Quinton, W. L., Shirazi, T., Carey, S. K., and Pomeroy, J. W.: Soil water storage and active-layer

development in a sub-alpine tundra hillslope, southern YukonTerritory, Canada, Permafrost Periglacial Processes, 16, 369–382, doi:10.1002/ppp.543, 2005.
Quinton, W. L., Hayashi, M., and Carey, S. K.: Peat hydraulic conductivity in cold regions and its relation to pore size and geometry, Hydrol. Process., 22, 2829–2837, doi:10.1002/hyp.7027, 2008.
Quinton, W. L., Elliot, T., Price, J. S., Rezanezhad, F., and Heck, R.: Measuring physical and hydraulic properties of peat from X-ray tomography, Geoderma, 153, 269–277, doi:10.1016/j.geoderma.2009.08.010, 2009.
Rezanezhad, F., Quinton, W. L., Price, J. S., Elrick, D., Elliot, T. R., and Heck, R. J.: Examining the effect of pore size distribution and shape on flow through unsaturated peat using computed tomography, Hydrol. Earth Syst. Sci., 13, 1993–2002, doi:10.5194/hess-13-1993-2009, 2009.
Serreze, M. C., Walsh, J. E., Chapin, F. S., Osterkamp, T., Dyurgerov, M., Romanovsky, V., Oechel, W. C., Morison, J., Zhang, T., and Barry, R. G.: Observational evidence of recent change in the northern high-latitude environment, Clim. Change, 46, 159–207, 2000.
Schlotzhauer, S. M. and Price, J. S.: Soil water flow dynamics in a managed cutover peat field, Quebec: Field and laboratory investigations, Water Resour. Res., 35, 3675–3683, 1999.
Smerdon, B. D. and Mendoza, C. A.: Hysteretic freezing characteristics of riparian peatlands in the Western Boreal Forest of Canada, Hydrol. Process., 24, 1027–1038, doi:10.1002/hyp.7544, 2010.
Smith, S. L, Burgess, M. M., Riseborough, D., Coultish, T., and Chartrand, J.: Digital summary database of permafrost and thermal conditions – Norman Wells pipeline study sites, GSC Open File 4635, 2004.
Stahli, M. and Stadler, D.: Measurement of water and solute dynamics in freezing soil columns with time domain reflectometry, J. Hydrol., 195, 352–369, 1997.
van Genuchten, M. T.: A closed-form equation for predicting the hydraulic conductivity of unsaturated soils, Soil Sci. Soc. Am. J., 44, 892–898, 1980.
Williams, P. J.: Properties and behavior of freezing soils, Norwegian Geotechnical Institute, Research paper # 359, 128 pp., 1967.
Wohlfarth, C.: Permittivity (Dielectric Constant) of Liquids, in: CRC Handbook of Chemistry and Physics, 91, edited by: Haynes, W. M., Taylor and Francis Group, LLC, 6-186-6-207, 2010.
Wright, N., Hayashi, M., and Quinton, W. L.: Spatial and temporal variations in active layer thawing and their implication on runoff generation in peat-covered permafrost terrain, Water



Discussion Paper | Discussion Paper | Discussion Paper | Discussion Paper |

Resour.Res., 45, W05414, 13 pp., 2009.
Zhang, Y., Carey, S. K., Quinton, W. L., Janowicz, J. R., Pomeroy, J. W., and Flerchinger, G. N.: Comparison of algorithms and parameterisations for infiltration into organic-covered permafrost soils, Hydrol. Earth Syst. Sci., 14, 729–750, doi:10.5194/hess-14-729-2010, 2010.





HESSD
8, 5387–5426, 2011



cc BY

**Table 1.** Details of the thickness (cm) of peat layers in each Mesocosm.

| Mesocosm | Undisturbed peat (top of core) | Repacked layer (middle of core) | Repacked frozen layer (bottom of the core) |
|---|---|---|---|
| M1 | 42 | 18 | 45 |
| M2 | 50 | 15 | 45 |
| M3 | 17 | 51 | 45 |
| M4 | 57 | 8 | 45 |





HESSD
8, 5387–5426, 2011



cc BY

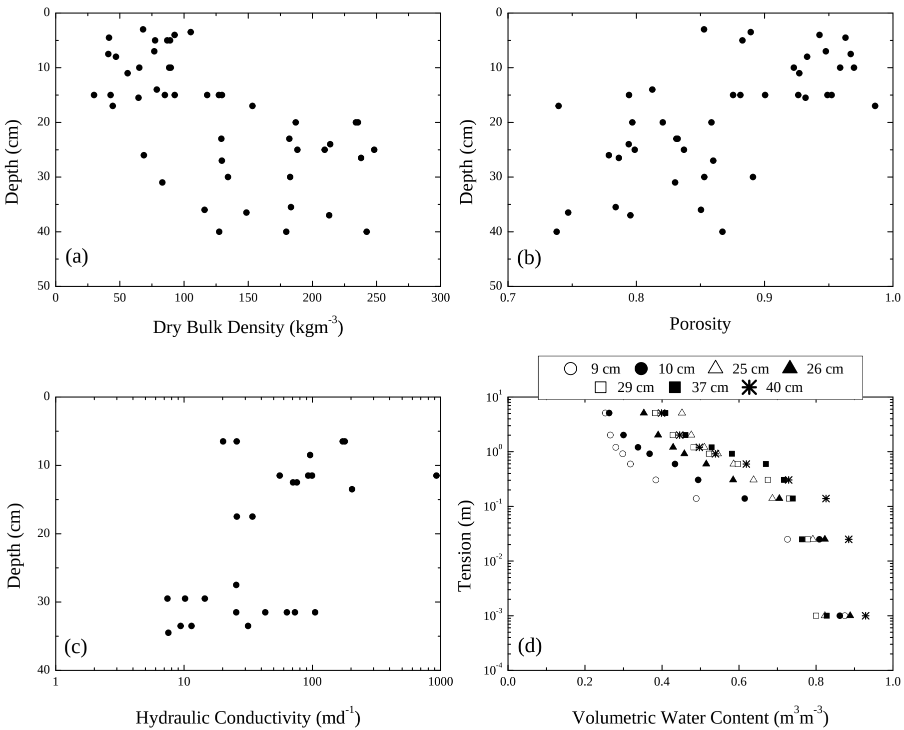


**Fig. 1.** Depth variation of **(a)** Bulk density (Hayashi et al., 2007), **(b)** porosity (Hayashi et al., 2007), **(c)** vertical hydraulic conductivity, and **(d)** soil water retention curves (Quinton and Hayashi, 2005) for peat from Scotty Creek watershed. The different symbols in **(d)** represent the samples taken at different depths as shown in legend.





HESSD
8, 5387–5426, 2011

Lab investigation of freezing processes in peat

R. M. Nagare et al.

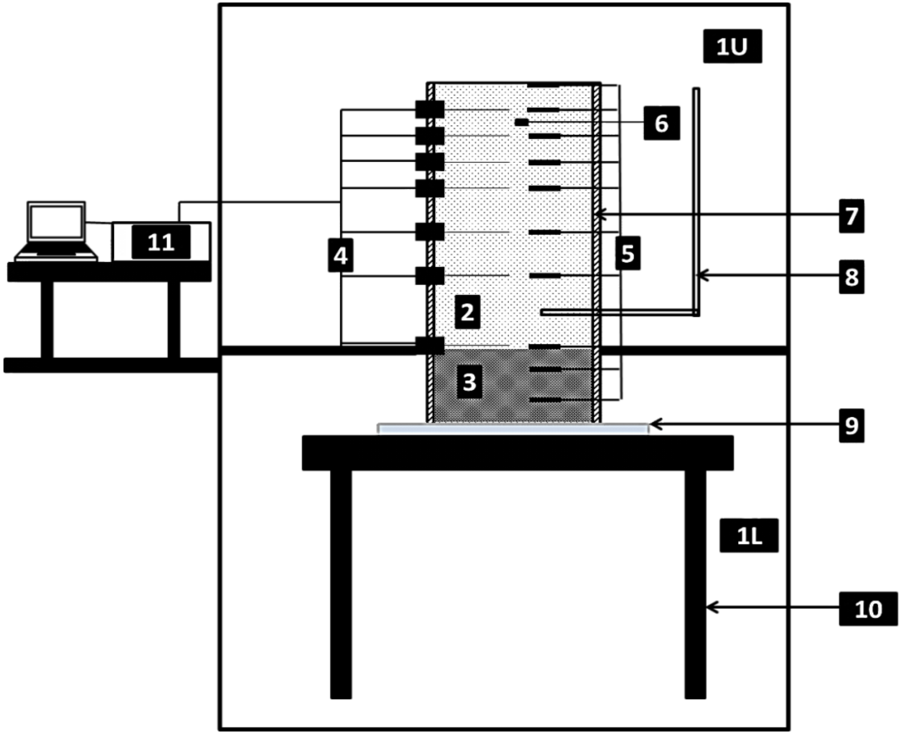


**Fig. 2.** Line diagram showing the experimental setup (from Nagare et al., 2011). 1U: Upper level chamber of the BESM; 1L: Lower level chamber of the BESM; 2: 65-75 cm deep unfrozen layer; 3: 45 cm bottom frozen layer (fully saturated before freezing); 4: TDR probes connected to 11 through low-loss coaxial cables; 5: temperature probes connected to 11; 6: heat flux plate; 7: LDPE container lined with neoprene from inside and insulated from outside; 8: stand pipe for water level measurements; 9: weighing scale; 10: custom made stand to support the entire experimental setup; 11: multiplexers and datalogger connected to a personal computer.





HESSD
8, 5387–5426, 2011

Lab investigation of freezing processes in peat

R. M. Nagare et al.

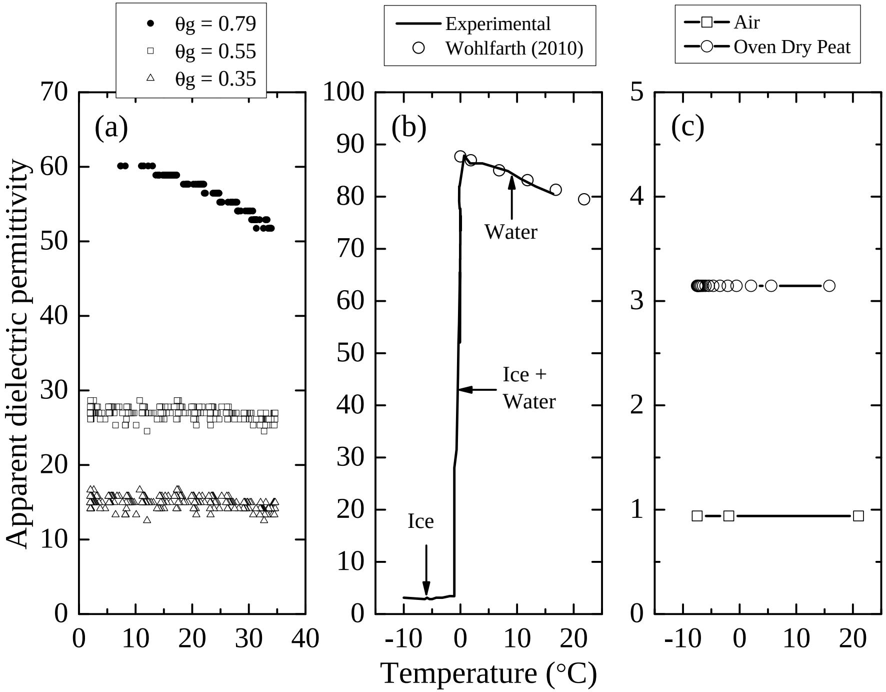


**Fig. 3.** **(a)** Effect of temperature on apparent dielectric permittivity measurements in peat (from Nagare et al., 2011). The gravimetric water content ($\theta g$) did not change over the duration of test. Effect of temperature on observed apparent dielectric permittivity of **(b)** water, and **(c)** air and oven dried peat as determined using TDR100. The dielectric constant of oven dried peat was derived from the bulk apparent dielectric permittivity using a 2-phase mixing formula.




CC BY

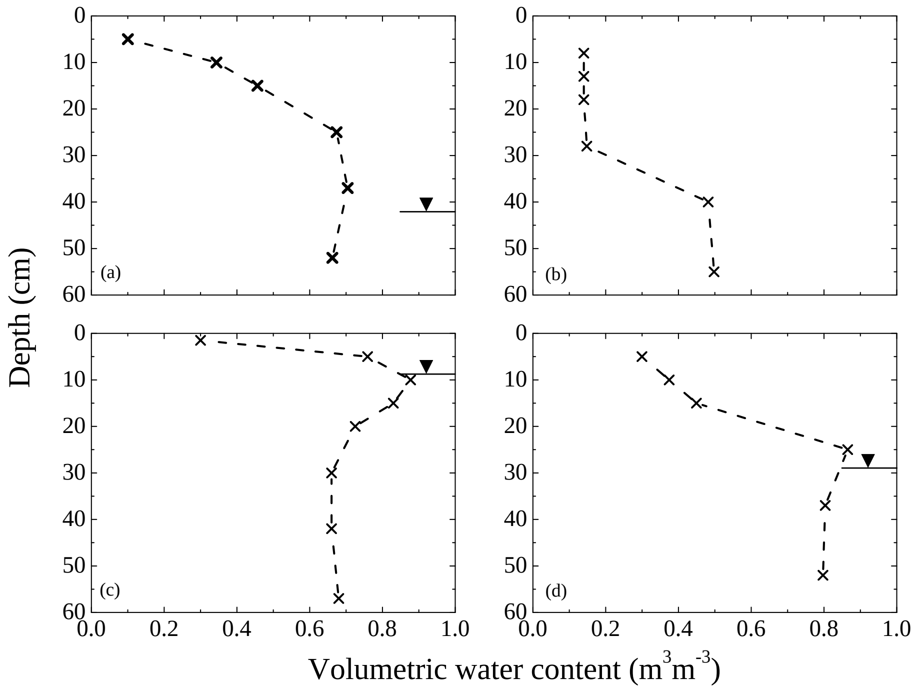


**Fig. 4.** Initial water content in Mesocosms **(a)** 1, **(b)** 2, **(c)** 3, and **(d)** 4 for second freezing run. The depth to the groundwater table is shown by free water surface symbol. Mesocosm # 2 was unsaturated throughout the depth for before the second freezing run.





CC BY

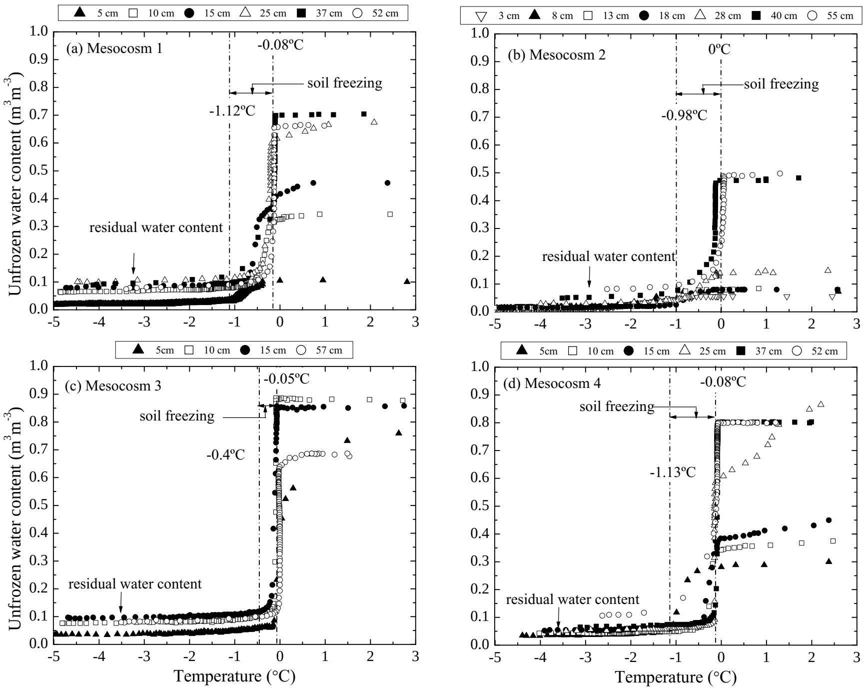


**Fig. 5.** Soil freezing characteristics of all four Mesocosms obtained from recorded unfrozen water and soil temperature data.

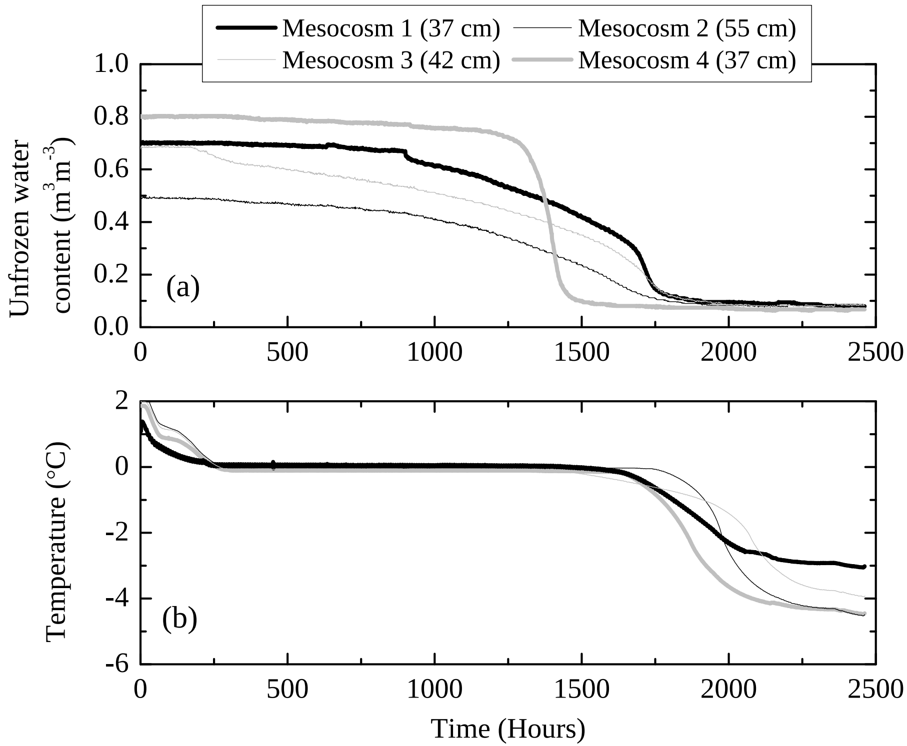


**Fig. 6.** **(a)** Soil unfrozen water content and **(b)** temperature time series at selected depths in the four Mesocosms. The depths were selected such that initial water content was greater than $0.5\,m^3\,m^{-3}$.





HESSD
8, 5387–5426, 2011

Lab investigation of freezing processes in peat

R. M. Nagare et al.

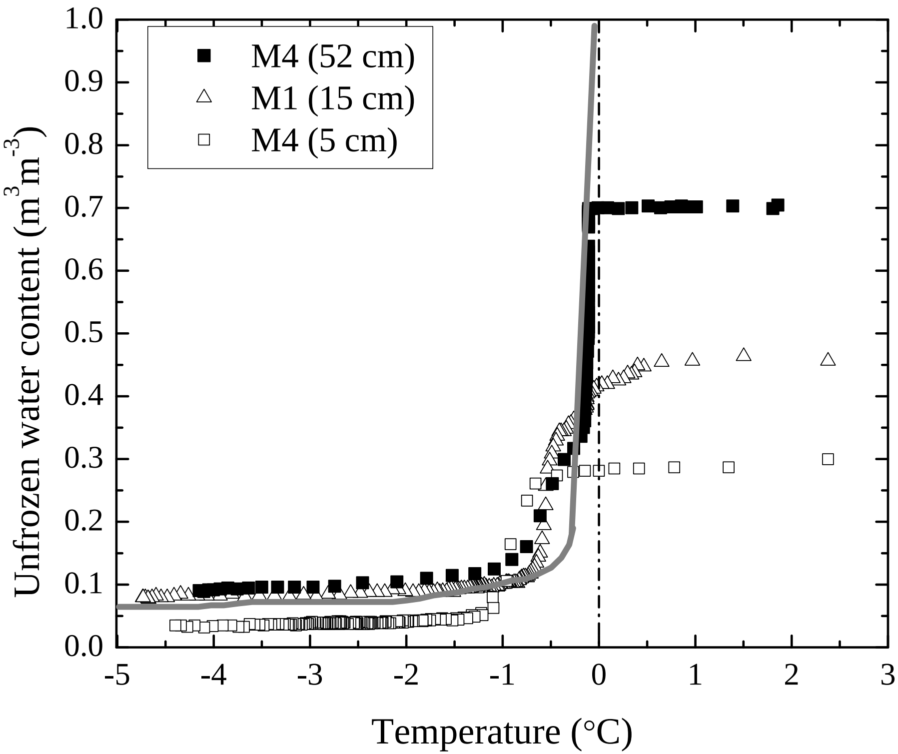


**Fig. 7.** Soil freezing curves in different Mesocosms (M1, M3 and M4). The effect of water redistribution on the shape of SFC is seen in form of deviation from an initial path the curves traverse (shown approximately by a thick gray line). The depth at which soil temperature-liquid water content relationship was observed is shown in parenthesis.





HESSD
8, 5387–5426, 2011

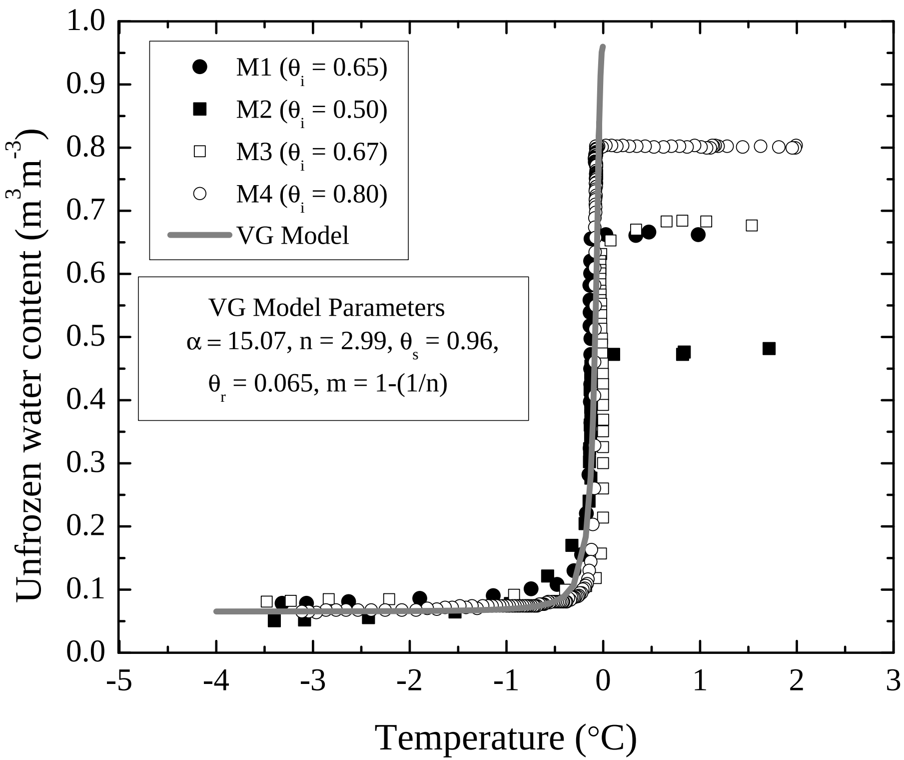


**Fig. 8.** Soil freezing curves chosen from four different Mesocosms and initially at different water contents ($\theta i$). A best fit defined by van-Genuchten model (VG Model, van Genuchten, 1980) is also shown along with the VG Model parameters. The SFC's were chosen from each Mesocosm such that $\theta i \geq 0.5\,m^3\ m^{-3}$.





CC BY

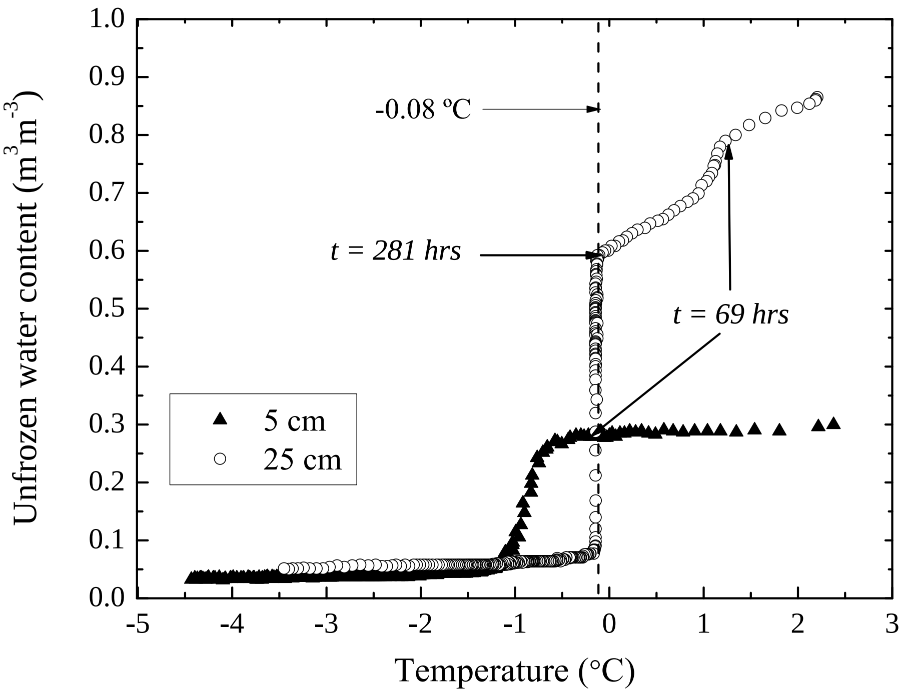


**Fig. 9.** Water movement towards freezing front: soil freezing characteristics of **(a)** Mesocosm 4 shows change in slope of the curve at 25 cm depth exactly when the freezing front reaches 5 cm depth.





HESSD
8, 5387–5426, 2011

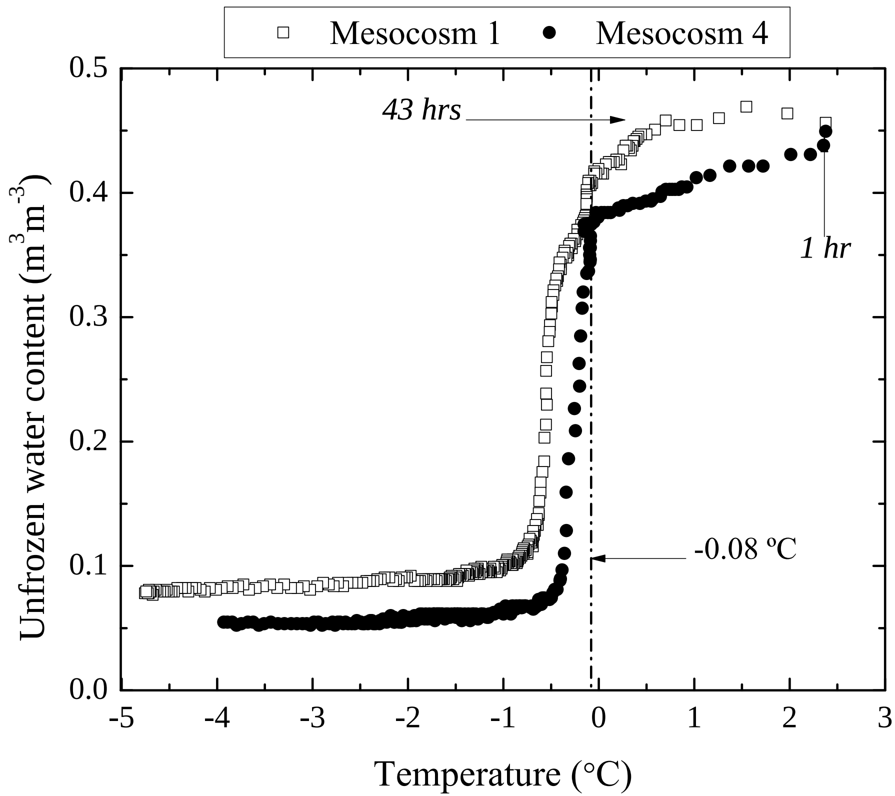


**Fig. 10.** Comparison between the soil freezing curves of Mesocosms 1 and 4 at 15 cm depth. This depth in both Mesocosms loses water before the soil temperature drops below freezing point, however M4 starts to lose water much earlier (1 h) than M1 (43 hours). Both Mesocosms were exposed to air temperature of −7.5 °C at the surface at time = 0 h.





CC BY

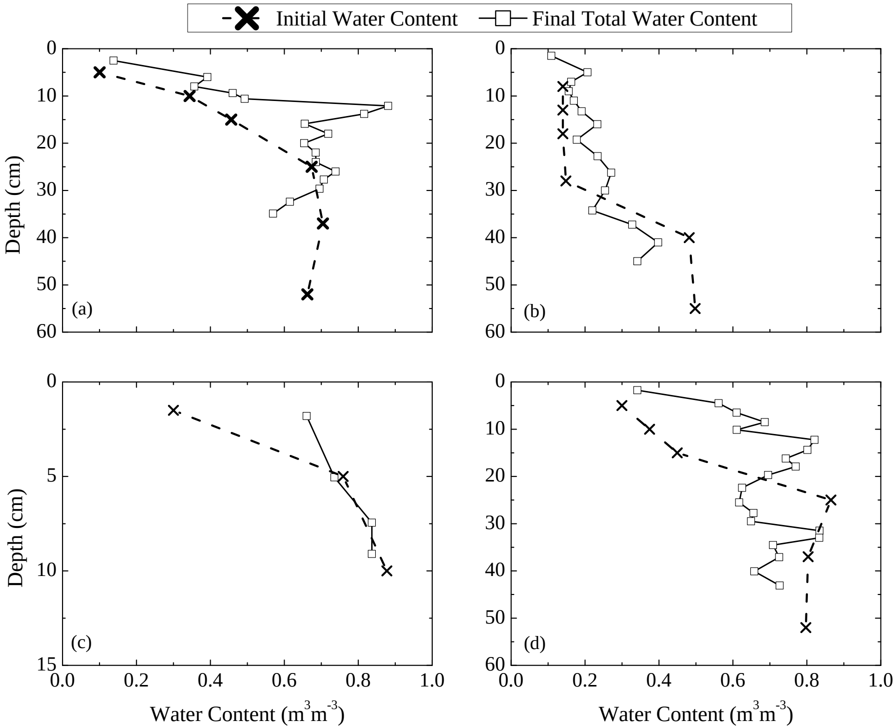


**Fig. 11.** Initial (liquid) and final (total) water content after 2000 h of freezing in Mesocosms **(a)** 1, **(b)** 2, **(c)** 3, and **(d)** 4. Please note the different Y-axis limits in **(c)**.





HESSD
8, 5387–5426, 2011

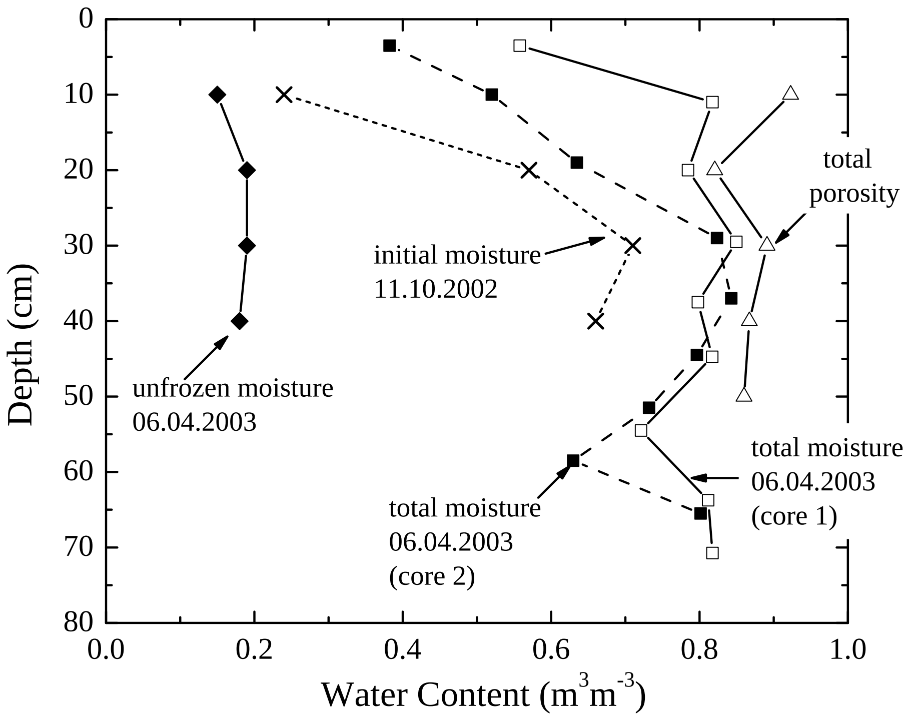


**Fig. 12.** Observed initial (liquid) and final water contents (liquid + ice) at Scotty Creek field site for winter of 2002–2003 (Quinton and Hayashi, 2008). The initial and unfrozen moisture content readings are from a soil pit being measured using a water content reflectometer. Two frozen cores were sampled at the end of winter season near the soil pit and total (liquid + ice) water content was determined gravimetrically.





HESSD
8, 5387–5426, 2011

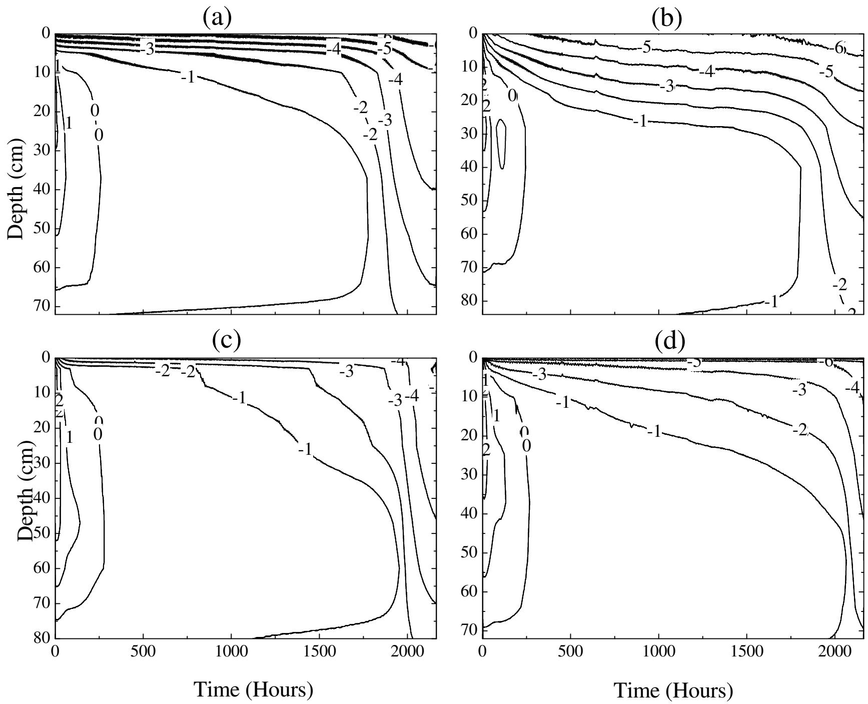


**Fig. 13.** Isolines of equal temperature across depth and time for **(a)** M1, **(b)** M2, **(c)** M3 and **(d)** M4.





HESSD
8, 5387–5426, 2011



CC BY

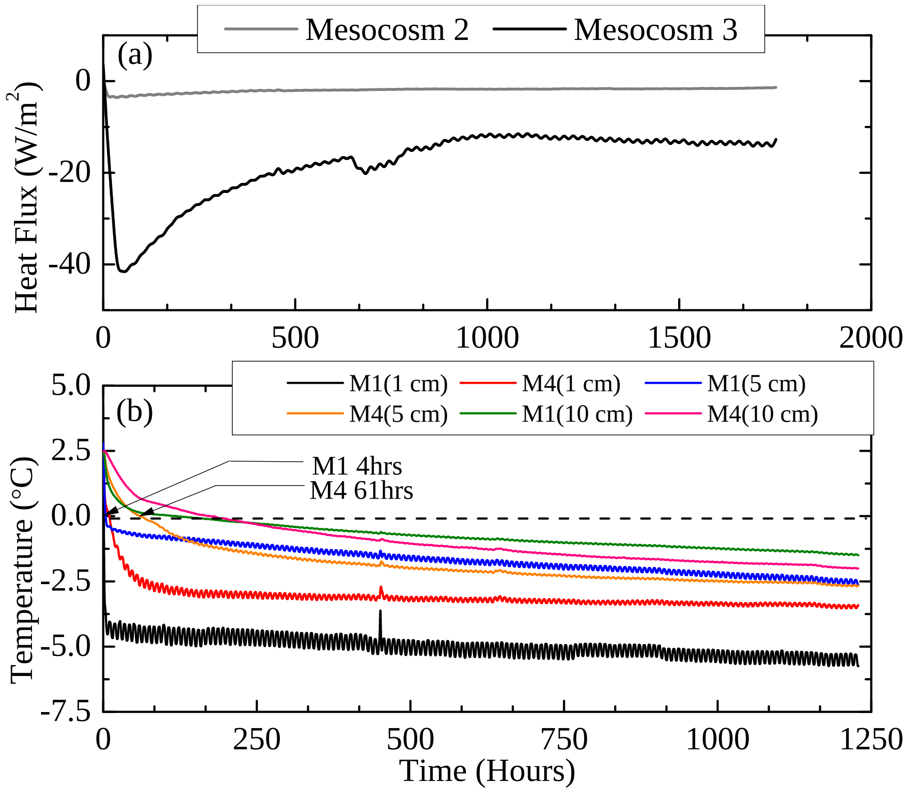


**Fig. 14. (a)** Observed ground heat flux in fully saturated M3 and dry M2 (at the start of freezing), and **(b)** Temperature time series for near surface sensors in Mesocosms M1 and M4. Note that the differences in time intervals.





HESSD
8, 5387–5426, 2011

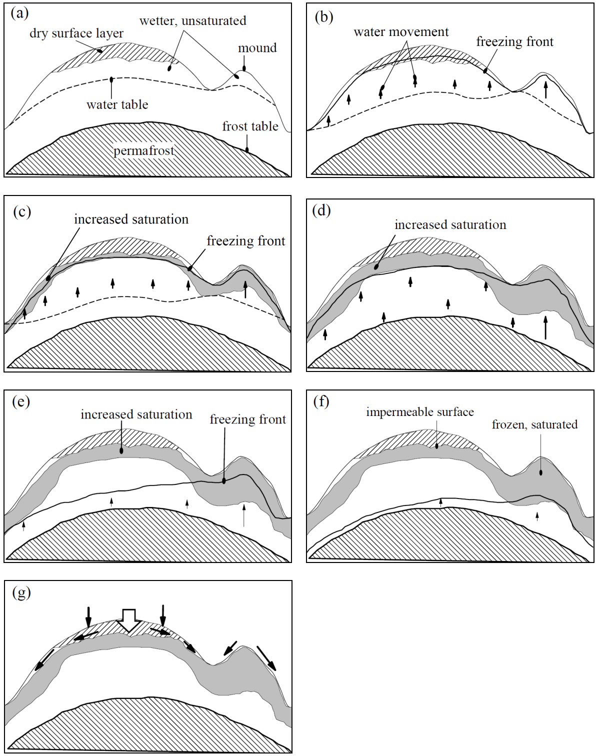


**Fig. 15.** Conceptual model describing freezing induced water redistribution and frost propagation inside an organic active layer on a peat plateau **(a)** onset of winter, **(b)** early winter, **(c)** early-mid winter, **(d)** mid winter, **(e)** and **(f)** mid-late winter, and **(g)** end of winter and spring runoff. Variable moisture landscape made up of regions with deeper unsaturated zones plus dry surface layer (zone of lower hydraulic conductivity) and shallow water table with wetter unsaturated zone (zone of higher hydraulic conductivity) result into variable amount of freezing induced moisture movement and different rates of freezing front movement.